Whole Powder Pattern Fitting: Rietveld and Pawley/Le Bail Methods

Prof. J.S.O. Evans (John), Department of Chemistry, Durham University, Lower Mount Joy, South Road, Durham, DH1 3LE, UK.

Prof. W.I.F. David (Bill), Inorganic Chemistry Laboratory, Department of Chemistry, University of Oxford, South Parks Road, Oxford, OX1 3QR, UK and ISIS Pulsed Neutron and Muon Facility, Rutherford Appleton Laboratory, Harwell Campus, OX11 0QX, UK.

Prof. R. E. Dinnebier (Robert), Max Planck Institute for Solid State Research, Heisenbergstraße 1, 70569 Stuttgart, Germany.

1. Introduction and overview

Previous lectures in the school have covered the fundamentals of scattering and powder diffraction; how to collect good quality experimental data and how to identify known phases from these data. We then learned how it is possible to begin to determine new crystal structures by indexing peaks in a powder diffraction pattern to obtain unit-cell parameters. Once the Bravais lattice and unit-cell parameters have been ascertained, the space-group symmetry can be determined through an analysis of systematic absences. The final stages in structure determination, the refinement of the crystal structure parameters involve (i) verifying the choice of unit cell and space group, (ii) obtaining a starting structural model and (iii) final structural refinement. Each of these stages rely on the quantitative analysis of intensity information in the powder pattern. This process runs up against the most widely discussed challenge of working with powder diffraction data: the accidental or non-accidental (e.g. the (300) and (221) reflections of a cubic sample) overlap of individual *hkl* reflections in the1D dataset. This makes the determination of individual I_{hkl} intensities difficult for accidental overlap and impossible for non-accidental overlap.

An effective solution to the overlap problem was reported in breakthrough papers in the late 1960s,[1-2] which described how the whole powder pattern could be simultaneously fitted point-by-point using (i) an empirical function to describe the background between Bragg peaks, (ii) peak positions constrained by unit-cell parameters, (iii) peak shapes described by simple empirical functions (initially Gaussian functions), (iv) reflection intensities described by a structural model that can be refined and (v) terms to describe any experimental aberrations (e.g. the diffractometer zero-point). This one-step process removed the need to extract individual intensities, and was formally called Rietveld analysis in 1978. A typical profile fit from a Rietveld analysis is shown in Figure 1.

Since that time similar methods have been developed for structure-independent fitting of powder patterns – most commonly using the Pawley[3] or Le Bail[4-5] methods. Freestyle methods can also be effective in early stages of the diffraction analysis where individual peaks may be fitted without the necessity of unit-cell determination. Approaches analogous to Rietveld analysis also underpin some structure solution methods, methods for quantitative analysis, as well as methods for extracting purely microstructural information from powder data. As the fitting process involved in many of these is similar, we will discuss them together under the collective term of “Whole Powder Pattern Fitting” (WPPF). We will follow the same sequence as the historical development of the methods and introduce ideas using structural (Rietveld) refinement before summarising the key differences in structure-independent methods. There are a number of excellent specialist texts that cover the method and its historical development in depth.[6-11] There is also a very useful set of Rietveld guidelines published by McCusker et al. in 1999.[12]

2. WPPF by least squares – a mathematical overview

At its core, WPPF is a constrained mathematical fitting challenge. The aim is to develop a model which describes all aspects of the powder diffraction pattern (background, peak positions, peak shapes and peak intensities) such that the information of interest can be extracted. In a classic Rietveld analysis, the structural model, consisting of atom positions, occupancies and thermal motion, determines the peak intensities as it is the structure that is of interest. In a Pawley or Le Bail analysis, it is the intensities that are of principal interest. In other analyses, such as microstructure determination, the significant information is mostly derived from the peak shapes.

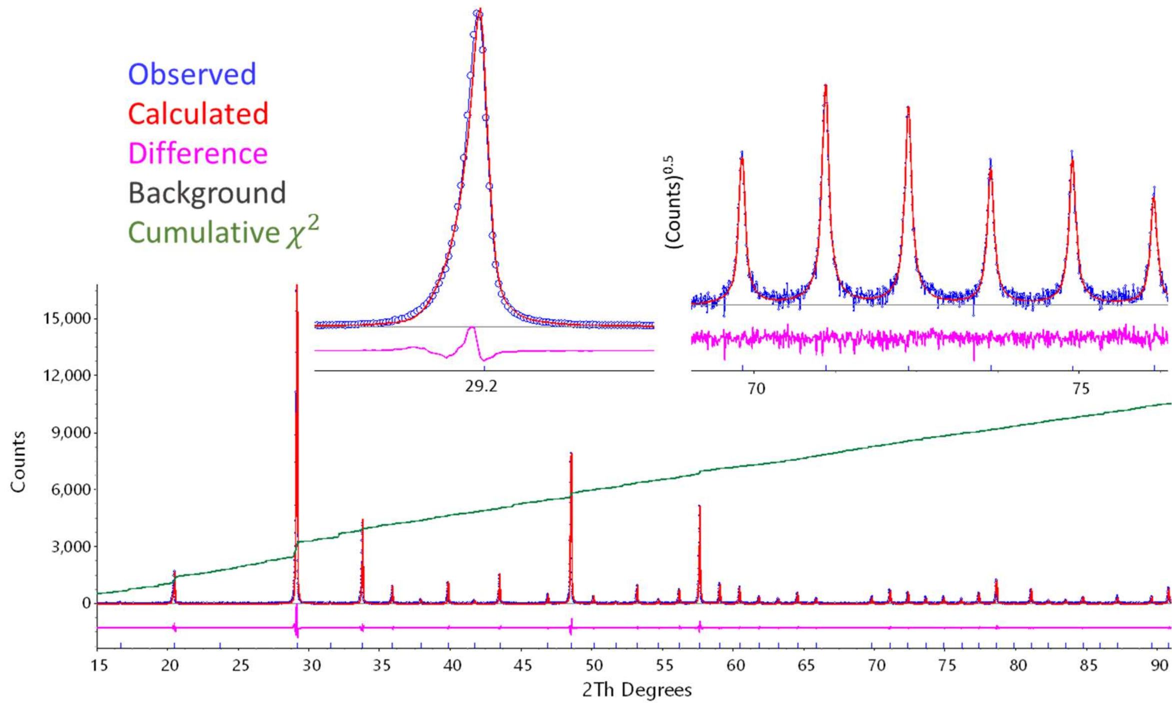

Figure 1: A typical fit to a powder diffraction pattern using the Rietveld method. Observed data are shown in blue, calculated in red and the difference in pink. The green line shows the cumulative-χ^2 and the grey line in the insets shows the fitted background. The high-angle inset is shown on a square root scale to emphasise weak features. Vertical blue tick marks show the calculated positions of different *hkl* reflections. See the text for discussion of all these quantities.

As discussed in previous lectures, a powder diffraction pattern can be obtained from a range of radiation sources (X-rays, neutrons, electrons) using a variety of sources (home-lab facilities, synchrotrons, neutron sources or XFEL facilities) and with different types of detectors. The diffraction pattern is generally reduced to a digital form of N consecutively measured intensities $y_{obs,i}$ at positions $X_{obs,i}$ where $i \in [1,..,N]$ and $X_{obs,i}$ might be diffraction angle 2θ, momentum transfer q, energy E, or time-of-flight. There will also be experimental uncertainties $\sigma(y_{obs,i})$ associated with each intensity. With a traditional point detector, Poisson statistics apply such that $\sigma(y_{obs,i}) = \sqrt{y_{obs,i}}$ For more complex experiments $\sigma(y_{obs,i})$ should be extracted as part of the data reduction process.

A general expression for the calculated intensity $y_{calc,i}$ at any point in a powder pattern of a multiphase sample is:

$$y_{calc,i} = \sum_{ph}\left(S_{ph}\sum_{\mathbf{s}(ph)}\left(\left|F_{calc,\mathbf{s},ph}\right|^2 \Phi_{s,ph,i} Corr_{\mathbf{s},ph,i}\right)\right) + Bkg_i \qquad \text{(Eq. 1)}$$

Here the outer sum runs over all the crystalline phases in the sample while the inner sum runs over each $\mathbf{s} = (hkl)$ reflection of phase ph which contribute significant intensity to position i in the pattern. $F_{calc,\mathbf{s},ph}$ is the calculated structure factor of the reflection, $\Phi_{s,ph,i}$ is the value of the profile function at point i relative to the position of the Bragg reflection, and $Corr_{\mathbf{s},ph,i}$ is the product of all the correction functions that need to be applied to relate the structure factor and the reflection intensity. Bkg_i describes the background at point i. Note that some points in the pattern might receive contributions from multiple *hkl* reflections (e.g. high q regions for complex structures with broad reflections) and some from none (low q, simple structures, sharp peaks). Similar expressions hold for Pawley and Le Bail fitting, but the structure factor and correction terms are no longer calculated from a structural model.

To fit the pattern, most Rietveld packages use least squares methods[13-14] to minimize the objective function S where:

$$S = \sum_{i=1}^{N} w_i \left(y_{obs,i} - y_{calc,i}(\mathbf{p})\right)^2 \qquad \text{(Eq. 2)}$$

In this expression $y_{calc,i}$ is shown as depending on the various parameters p_j in the model via the parameter vector $\mathbf{p}$. The vector will look like:

$$\mathbf{p} = \begin{pmatrix} p_1 \\ \vdots \\ p_P \end{pmatrix} \qquad \text{(Eq. 3)}$$

and has size P, where P is the number of independent parameters in the model. In a least squares fit the weights w_i in Eq. 2 are related to the experimental uncertainties by $1/\sigma\left(y_{obs,i}\right)^2$.

If the function $y_{calc,i}(\mathbf{p})$ were linear, then the parameters giving the minimum value of S in Eq. 2 (our best-fit model) could be directly obtained using standard mathematical tools – the problem is analogous to fitting the linear function $y = mx + c$ to a set of (x, y) data points. Unfortunately, the equations in diffraction are more complex and we need to adopt a non-linear iterative fitting approach.

For non-linear least squares we require an initial set of estimated starting parameters $p_1 \dots p_P$ (our "starting model"). In structural analysis, these parameters may be obtained from materials with similar structures, or from the structure solution methods discussed by Prof. McCusker. Since $y_{calc,i} = f(p_1, p_2, \dots, p_P)$, we can use the starting parameters to calculate $y_{calc,i}$ for each point in the pattern. Unless we are exceptionally fortunate, these parameters will not give the lowest value of $(y_{obs,i} - y_{calc,i})^2$ at each point i; S will not be minimised and, consequently, the model is not correct.

The mathematics underlying non-linear least squares is as follows: if we knew how much to change each parameter by (Δp_j) such that $y_{obs,i} - y_{calc,i}$ became as close-to-zero as possible, we could simply apply these Δp shifts to the starting model to find the best-fit model. With this in mind, we can express the change in intensity on changing parameters from an initial estimate $\mathbf{p_0}$ to $\mathbf{p}$ using a Taylor series (with just the first terms retained) as:

$$y_{calc,i}(\mathbf{p}) \approx y_{calc,i}(\mathbf{p_0}) + \left(\frac{\partial y_{calc,i}}{\partial p_1}\right)\Delta p_1 + \left(\frac{\partial y_{calc,i}}{\partial p_2}\right)\Delta p_2 + \cdots + \left(\frac{\partial y_{calc,i}}{\partial p_P}\right)\Delta p_P \qquad \text{(Eq. 4)}$$

and try to determine not the parameters but the parameter shifts $\mathbf{\Delta p} = \mathbf{p} - \mathbf{p_0}$. This turns a non-linear optimisation into a series of small linear steps.

Combining Eq. 2 and Eq. 4, the objective function can be written as:

$$S = \sum_{i=1}^{N} w_i \left(y_{obs,i} - \left(y_{calc,i}(\mathbf{p_o}) + \sum_{j=1}^{P} \frac{\partial y_{calc,i}(\mathbf{p_o})}{\partial p_j} \Delta p_j \right) \right)^2 \qquad \text{(Eq. 5)}$$

To find the minimum we need the first derivative with respect to the refined parameters, and we introduce subscript k to avoid confusion:

$$\frac{\partial S}{\partial p_k} = -2 \sum_{i=1}^{N} w_i \left(y_{obs,i} - \left(y_{calc,i}(\mathbf{p_o}) + \sum_{j=1}^{P} \frac{\partial y_{calc,i}(\mathbf{p_o})}{\partial p_j} \Delta p_j \right) \right) \frac{\partial y_{calc,i}(\mathbf{p_o})}{\partial p_k}$$

$$\text{(Eq. 6)}$$

$$= -2 \sum_{i=1}^{N} w_i \left(\left(y_{obs,i} - y_{calc,i}(\mathbf{p_o}) \right) \frac{\partial y_{calc,i}(\mathbf{p_o})}{\partial p_k} - \sum_{j=1}^{P} \frac{\partial y_{calc,i}(\mathbf{p_o})}{\partial p_j} \frac{\partial y_{calc,i}(\mathbf{p_o})}{\partial p_k} \Delta p_j \right)$$

Since $\frac{\partial S}{\partial p_k} = 0$ at the minimum, it follows that:

$$\sum_{i=1}^{N} w_i \sum_{j=1}^{P} \frac{\partial y_{calc,i}(\mathbf{p_o})}{\partial p_j} \frac{\partial y_{calc,i}(\mathbf{p_o})}{\partial p_k} \Delta p_j = \sum_{i=1}^{N} w_i \left(y_{obs,i} - y_{calc,i}(\mathbf{p_o})\right) \frac{\partial y_{calc,i}(\mathbf{p_o})}{\partial p_k} \qquad \text{(Eq. 7)}$$

Changing the summations on the left side leads to:

$$\sum_{j=1}^{P} \sum_{i=1}^{N} w_i \frac{\partial y_{calc,i}(\mathbf{p_o})}{\partial p_j} \frac{\partial y_{calc,i}(\mathbf{p_o})}{\partial p_k} \Delta p_j = \sum_{i=1}^{N} w_i \left(y_{obs,i} - y_{calc,i}(\mathbf{p_o})\right) \frac{\partial y_{calc,i}(\mathbf{p_o})}{\partial p_k} \qquad \text{(Eq. 8)}$$

This equation is linear in the parameter shifts $\Delta\mathbf{p}$. There will be one equation for each p_k and the set of equations can be concisely expressed in matrix notation as:

$$\mathbf{A}\Delta\mathbf{p} = \mathbf{Y} \qquad \text{(Eq. 9)}$$

with the components of the $P \times P$ matrix $\mathbf{A}$ (each k corresponds to a matrix row and each j corresponds to a column) given by:

$$A_{kj} = A_{jk} = \sum_{i=1}^{N} w_i \frac{\partial y_{calc,i}(\mathbf{p_o})}{\partial p_j} \frac{\partial y_{calc,i}(\mathbf{p_o})}{\partial p_k} \qquad \text{(Eq. 10)}$$

and the P components of the vector $\mathbf{Y}$ by:

$$Y_p = \sum_{i=1}^{N} w_i \left(y_{obs,i} - y_{calc,i}(\mathbf{p_o})\right) \frac{\partial y_{calc,i}(\mathbf{p_o})}{\partial p_k} \qquad \text{(Eq. 11)}$$

The equations in Eq. 9 are called the normal equations of least squares and can be solved by pre-multiplying each side of the equation by $\mathbf{A}^{-1}$ to give the parameter shifts $\Delta\mathbf{p}$ which should be applied to the model.

$$\mathbf{A}^{-1}\mathbf{A}\Delta\mathbf{p} = \Delta\mathbf{p} = \mathbf{A}^{-1}\mathbf{Y} \qquad \text{(Eq. 12)}$$

In practice the approximations made in the Taylor series of Eq. 4 mean that this recipe is not perfect and won't immediately give the best-fit model. The process is therefore iterated multiple times, ideally with an improvement between $y_{calc,i}$ and $y_{obs,i}$ on each iteration. The process is stopped when no further improvement is observed in the fit (i.e. there is no significant reduction in S), or the parameter shifts become comparable to their uncertainties. These uncertainties, and the covariance between different parameters, can be extracted from the inverse matrix $\mathbf{A}^{-1}$ normalized by the reduced χ^2. (Eq. 26 later). Critical analysis of this variance-covariance matrix to assess model reliability is a crucial part of all WPPF methods.

Much of the work of WPPF software goes into the manipulation of the matrices in Eq. 9 and solution of the normal equations. Modern software packages incorporate a number of mathematical tools to ensure that the fit improves on each cycle and that the refinement doesn't diverge due to mathematical instabilities. Some programs issue warnings about the determinant of matrices being small. These are flagging that the least squares process is unstable. A small determinant of the $\mathbf{A}$ matrix means large values in $\mathbf{A}^{-1}$ and therefore large uncertainties in the refined parameters.

3. Constraints and restraints

The useful information content of a powder diffraction pattern is often low due to peak overlap or a limited X range. In these cases it may be helpful to include extra information in the refinement in the form of *constraints* or *restraints* (sometimes confusingly called "soft constraints").

Constraints are strict instructions imposed on the refined model. For example, when refining the structure of an organic compound you might force a benzene ring to be a rigid hexagon with an edge of 1.39 Å surrounded by ideally placed hydrogens, and just refine its position and orientation in the unit cell. This reduces the number of parameters from 36 to 6. For an inorganic material you might want to force a ZrO_6 group to be a perfect octahedron. Symmetry operators imposed by the space-group symmetry are another form of constraint. For example, in a *C*-centred cell if there is an atom at (*x*, *y*, *z*) then there must be another at (*x*+½, *y*+½, *z*). Constraints are built into the left-hand side of Eq. 9 by changing the equations that are solved. This ensures appropriate parameter shifts are applied to the model such that the constraints are obeyed.

Restraints are softer pieces of information used to guide a refinement. In the benzene case you might restrain all C–C bonds to be equal, all C–H bonds to be equal and the atoms to be approximately co-planar; instead of using a rigid ZrO_6 octahedron you might introduce restraints that all the Zr–O bonds are around 2.075 Å and the O–Zr–O angles are close to 90° or 180°. Mathematically the restraints are treated like extra experimental observations and appear on the right-hand side of Eq. 9. The quantity minimized by least squares then becomes:

$$\chi^2_{\text{total}} = \chi^2_{\text{data}} + weight \times \chi^2_{\text{restraints}} \qquad \text{(Eq. 13)}$$

with some weighting between the two contributions. χ^2_{data} is related to the least squares objective function and defined later in Eq. 26. $\chi^2_{\text{restraints}}$ can be expressed in multiple ways but will often contain terms like $(d_{\text{ideal}} - d_{\text{model}})^2$, which reduce to zero when the distance in the model equals the ideal value. Some software packages use the term "penalties" and "restraints" for subtly different ways in which this type of idea is applied.

Most software packages will apply an appropriate overall weighting between χ^2_{data} and $\chi^2_{\text{restraints}}$. The $\chi^2_{\text{restraints}}$ term can, however, contain multiple contributions (distance restraints, angle restraints, planar restraints, occupancy restraints, etc.). The relative weighting of these is typically set by the user based on their scientific judgement. It is important that the relative and overall weights are set appropriately. If the overall weighting of restraints is too high, then the refinement will obey them in preference to fitting the data (in the limit they behave like constraints). There is no value in reporting a refined Zr–O distance of 2.075 Å if that value is forced by a user-restraint. Information on restraints and their weighting should be included in any publication.

4. Quantities typically refined in WPPF

The parameters refined in WPPF can be separated in various ways. One is to split them into contributions from the instrument and sample as in Table 1. Another is to separate them into parameters that influence the four main information regions of a powder pattern: the background, the peak positions, the peak shapes, and the peak intensities. We will follow this latter approach and discuss a few WPPF-relevant points on each.

4.1 Background

In most WPPF analyses the background between Bragg peaks is not of direct interest (though it is crucially important in PDF or diffuse scattering work).[15-16] It is most commonly fitted using a smoothly varying function such as a Chebyshev polynomial or a cosine Fourier series. In the early days of the Rietveld method, the background was described manually via straight-line segments between fixed points; this approach is rarely used nowadays. If there is a significant background contribution due to the sample environment, it is good practice to measure this separately and either subtract it (often in fitted form) from the experimental data or include it as an extra fitted quantity during refinement. If the origin of the

background is well understood (e.g. diffuse scattering due to a capillary or from specific disorder in the sample) it can be described using simple analytical functions. Ideally a function (or combination of functions) should be chosen that fits the observed background to within experimental uncertainty and doesn't correlate with parameters of interest. Visualising fits on a $\sqrt{y}$ scale can help assess the quality of a background model.

Table 1: Selection of instrumental and sample effects influencing position (as a shift) and/or intensity (as a correction factor) and/or peak shape (as a convolution) of the Bragg reflections which might be included in a Rietveld refinement. Adapted from the text by Dinnebier, Leineweber and Evans.[7]

Instrument factors				**Sample factors**			
	Pos'n (shift)	**Int. (factor)**	**Profile (convolution)**		**Pos'n (shift)**	**Int. (factor)**	**Profile (convolution)**
Zero shift	x			Linear absorption/ transparency	x	x	x
Specimen displacement	x			Surface roughness		x	
Equatorial divergence (fixed slit)			x	(An)isotropic microstrain			x
Equatorial divergence (variable slit)		x	x	(An)isotropic crystallite size			x
Size of source (equatorial plane)			x	Preferred orientation		x	
Specimen tilt			x	Extinction		x	
Receiving slit length (axial plane)			x	Overspill		x	
Receiving slit width (eq'l plane)			x	Reflection multiplicity		x	
Emission profile		x	x	Phase fraction		x	
Tube tails			x	Fractional atomic coordinates		x	
Axial divergence (Sollers etc)	x		x	Site occupancy		x	
Lorentz-polarization		x		Displacement parameter		x	

4.2 Peak positions

As discussed elsewhere in the school, the peak positions in a powder pattern are influenced by many factors. The most important structure-related parameters are the unit-cell parameters, which should usually be refined in whole-pattern fitting. They are typically very well defined by a good powder experiment and indeed are usually superior to single crystal diffraction values. They also do not correlate strongly with other structural parameters. Instrumental effects such as the zero-point shift, sample height or offset errors and sample transparency (in Bragg-Brentano geometry) will also shift peak positions and corrections for these are often refined. One of the most common "Rietveld crimes" is failing to realise that these correction terms can be highly or, indeed, completely correlated with one another and with the unit-cell parameters. For example, while the 2θ dependence of a zero-shift and sample-height correction differ for a Bragg-Brentano measurement, they normally cannot be refined simultaneously. On a well-maintained lab instrument height errors normally dominate peak shifts. On synchrotron powder diffractometers, the asymmetry correction associated with the finite sample size correlates strongly with the unit-cell parameters and the zero-point.

To obtain both precise and accurate unit-cell parameters it is crucial to treat factors leading to peak asymmetry and peak maxima shifts correctly. This is particularly true with the inherently asymmetric peaks in time-of-flight neutron data. One effective approach is to fit an external or internal standard such

as NIST Si with fixed cell parameters, determine any corrections required, then apply identical corrections to the sample of interest. Parameters such as the wavelength of X-ray radiation and flight-path-length-related calibration constants of time-of-flight diffractometers scale linearly with cell parameters, so must not be refined simultaneously!

4.3 Peak shapes

As discussed elsewhere in the course, the peak shape observed in a powder diffraction experiment is a combination (strictly a convolution) of effects due to the instrument and the sample:

$$overall_peak_shape = (instrument \otimes sample)(X) \qquad \text{(Eq. 14)}$$

The instrumental contribution is often called the *instrumental resolution function* (IRF). There are multiple contributions to both the instrumental and sample terms, and they combine to give a profile that can vary in width, shape and asymmetry as a function of *X*.

In the earliest Rietveld refinements, which used low resolution constant wavelength neutron data, Gaussian functions were used to model the peaks. The 2θ-dependence of their full width at half maximum (*fwhm*) was described using expressions such as:

$$gauss_fwhm = \sqrt{U \tan^2 \theta + V \tan \theta + W} \qquad \text{(Eq. 15)}$$

with *U*, *V* and *W* refinable parameters (the Cagliotti function).[17] For laboratory X-ray data, it is common to include a Lorentzian component to the peak shape with a *fwhm* described by expressions such as:

$$lor_fwhm = X/\cos \theta + Y \tan \theta \qquad \text{(Eq. 16)}$$

Gaussians and Lorentzians can be described with the expressions:[11]

$$G = \frac{C_0^{1/2}}{fwhm \cdot \pi^{1/2}} \exp\left(\frac{-C_0(2\theta_i - 2\theta_{hkl})^2}{fwhm^2}\right) \qquad \text{(Eq. 17)}$$

$$L = \frac{C_1^{1/2}}{fwhm \cdot \pi} 1 \Big/ \left[1 + C_1 \frac{(2\theta_i - 2\theta_{hkl})^2}{fwhm^2}\right] \qquad \text{(Eq. 18)}$$

where $C_0 = 4 \ln 2$, $C_1 = 4$ and $2\theta_{hkl}$ is the ideal peak position.

Nowadays, the most commonly-used *empirical peak shapes* in Rietveld fitting of constant wavelength data are Voigtian or pseudo-Voigt functions. A Voigt is a convolution of a Gaussian and Lorentzian. The simplest expression of a pseudo-Voigt is a linear mixing of a Gaussian and Lorentzian: $PV = \eta L + (1 - \eta)G$ with η a mixing coefficient ($0 \leq \eta \leq 1$). Many Rietveld packages use the Thompson-Cox-Hastings (TCHz) pseudo-Voigt function which includes an additional $Z/\cos^2 \theta$ term in Eq. 15, and where the mixing component is not refined but is set by the combination of the refinable parameters *U*, *V*, *W*, *Z*, *X* and *Y*.[18] Whilst this is often treated as a purely empirical function, the 2θ dependence of some of the terms are related to size ($1/\cos \theta$) and strain ($\tan \theta$) effects in the sample. A wide variety of other empirical peak shape functions have been employed in different software packages, and details can be found in the literature.[6-7, 11]

At the other extreme to this empirical approach, peak shapes can be described using the so-called *fundamental parameters approach*. Here the contribution of every aspect of the instrument (radiation source, slits, collimators, detectors, sample geometry, etc) and sample (size, strain, faults, transparency, thickness, etc.) to the peak shape is modelled using a physically meaningful function.[19-25] This can allow the description of remarkably complex peak shapes with a small number of refinable parameters. Separating the contributions from the sample and instrument can also allow the extraction of meaningful information about microstructure.

A half-way house between these two extremes is a *semi-empirical* approach whereby the IRF is measured using a highly crystalline, strain-free sample (often LaB_6 or annealed CeO_2 on a lab instrument). This is the authors' standard approach. The peaks of this standard are then fitted with any combination of empirical and fundamental-parameters-like expressions that are needed. When a sample of interest is analysed, the parameters of the empirical IRF are fixed, and sample-specific functions convoluted on top. This approach again allows complex peak shapes to be well-fitted with a small number of refined parameters.

It is also common that real materials have *hkl*-dependent peak shapes due to strain, size or specific structural faults. These show up most commonly in high resolution synchrotron measurements, where the contribution of the IRF to the overall peak shape is low. Many Rietveld packages offer ways to describe these effects. Approaches include the Stephens and Popa models for anisotropic strain broadening,[26-27] symmetry-adapted spherical harmonics to allow a *hkl*-specific *fwhm*, or specific faulting models.[7, 28]

The application and analysis of peak shapes is, again, a complex area and there are numerous traps to fall into. Perhaps the most common is that high correlation between peak profile coefficients can lead to the least squares getting trapped in false minima or diverging. In fact, some common peak shape parameters are infinitely correlated (e.g. the combination of U, W, and Z in the TCHz function) and should never be refined together. One should also be very careful when using *hkl*-dependent peak shapes that the apparent improvement in fit is not just "mopping up" a more fundamental error in the structural model.

Finally, it is important to be pragmatic about peak shapes. While in some analyses it is critically important to describe the peak shape "perfectly", this is not always the case. For example, in most structural work, the minor misfits in peak shapes will not affect the relative intensities of reflections that influence structural parameters provided the misfit is similar for all reflections (though a lower χ^2 due to better fitting will influence uncertainty estimates).

5. Peak intensities

5.1 Pawley and Le Bail methods

In a Pawley or Le Bail analysis, the intensities of individual reflections are freely refined to give the best agreement between observed and calculated patterns. For the Pawley method, the expression is identical in form to Eq. 2. For the Le Bail method, the function is based around minimising the modulus of the weighted difference between observed and calculated diffraction data. If the purpose is to check that all the experimentally observed peaks are adequately predicted by the cell and space-group combination, then the intensity terms in Section 5.3 do not need to be applied. If quantitative intensities are needed for structure solution or as part of quantitative phase analysis then they should be.

One useful aspect of the Pawley and Le Bail methods is that the final R_{wp} agreement factor (see Section 6) gives a target for an eventual Rietveld. Mathematically, the more constrained Rietveld analysis cannot give a better goodness of fit than a Pawley analysis; the Pawley therefore gives a data set-specific target.[29]

5.2 Rietveld analysis

In the Rietveld method, peak intensities are determined or constrained by the crystallographic model. The general expression for the intensities has been covered previously but can be given as:

$$I_{calc,\mathbf{s}} = scale \times m \times LP \times |F_{calc,\mathbf{s}}|^2 \times other\ corrections \quad \text{(Eq. 19)}$$

where $scale$ is an overall scale factor, m is reflection multiplicity, LP describes the Lorentz-polarisation correction, and $F_{calc,\mathbf{s}}$ the calculated structure factor for reflection $\mathbf{s} = hkl$. $F_{calc,\mathbf{s}}$ is given by:

$$F_{calc,s} = \sum_j t_j \times occ_j \times f_j \times \exp[2\pi i(hx_j + ky_j + lz_j)] \quad \text{(Eq. 20)}$$

As in any crystallographic analysis, intensities are therefore affected by the fractional atomic coordinates (x_j, y_j, z_j) of the j atoms, the occupancy of sites (via the scattering factor f_j and occupancies, occ_j) and the atomic displacement parameters (t_j).

Due to the low number of experimental observations in many powder patterns one typically has to be cautious with the parameters refined. The sensitivity to a light atom position (e.g. H in an organic molecule or O in a heavy metal oxide) may be low with X-ray data. In these cases use of neutron data or a combined X-ray and neutron refinement might be appropriate. Similarly, one might need to restrict analysis to a small number of isotropic displacement parameters (a single overall parameter or one per atom type). With neutron data, where the point scattering of neutrons gives high intensity data over a larger q-range, the use of anisotropic displacement parameters may be possible or even necessary for some analyses.

The most common Rietveld "crime" related to intensities is to refine parameters that are not supported by the data. For example, with data over a narrow q-range, site occupancies and atomic displacement parameters are often sufficiently correlated that they cannot be determined independently. As a corollary, it is wise to fit as large a range as feasible. For example, the almost absence of structure high scattering angle data is no reason not to include it in the analysis. Quite the contrary. Refining from low to high angle data particularly helps de-correlate thermal motion/disorder from site occupancy. It is also important to realise that (powder) diffraction measurements can be completely insensitive to some aspects of structure. Some examples include:

- The diffraction pattern of a hypothetical stoichiometric rock-salt-structured TiO would be indistinguishable from that of the true $Ti_{0.83}O_{0.83}$ vacancy-containing composition. In a Rietveld analysis, they would differ only by a scale factor, and the method is blind to the most interesting aspect of this structure.
- Similarly, for a metal oxide MO with three possible cations on the M site $(A_{1-x-y}B_xC_y)O$, diffraction is only sensitive to the relative scattering from M and O sites and the values of x and y cannot be determined without more information.
- Perovskites with general composition $A_{1-x}A'_xB_{1-y}B'_yO_{3-\delta}$ are of huge technological importance. Despite the simplicity of the basic structure, it is impossible to determine the values of x, y and δ from a single diffraction pattern for similar reasons. Prior elemental analysis, however, can help inform and constrain the model.
- The magnetic moment of neutrons means that Rietveld fitting of neutron data can be used for magnetic structure determination. Depending on the symmetry, it may not be possible to unambiguously determine moment direction. There are also a number of cases where very different magnetic structures have identical powder patterns. One example is shown in Figure 2.

5.3 Other intensity corrections

There are numerous other factors relating to the diffractometer set-up and sample that influence experimental intensities (see earlier lectures and Table 1). Many of these are routinely included in WPPF refinements. Effects such as sample absorption, surface roughness in a Bragg-Brentano measurement, extinction and beam overspill can be described using simple analytical functions, and coefficients of these might be refined during the analysis. Many of these will be highly correlated with site occupancies and atomic displacement parameters, as well as with each other so care must be taken.

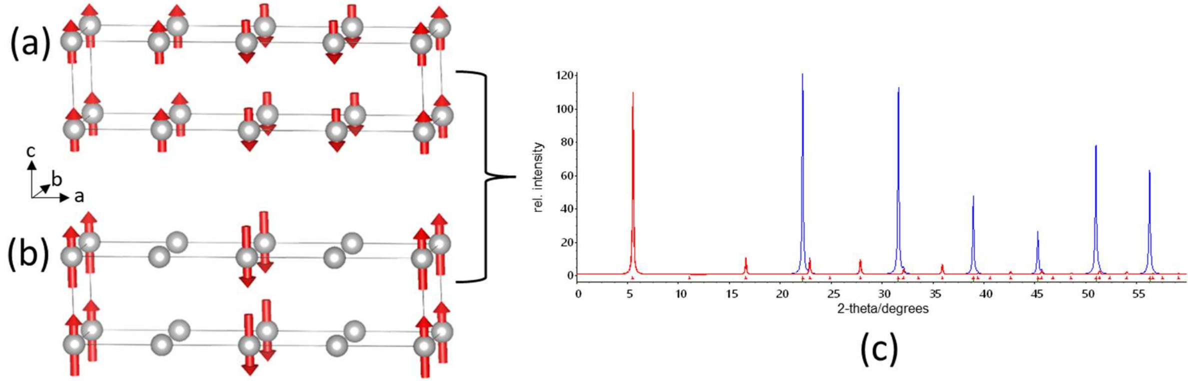

Figure 2: Two different magnetic structures in (a) and (b) that give rise to identical neutron powder diffraction patterns (c). The magnetic moment in (b) is $\sqrt{2}$ that in (a). The magnetic contribution to the pattern is shown in red on top of the total pattern in blue.

In Rietveld refinement it is often possible to account for preferred orientation effects with a small number of refinable parameters using either a March–Dollase[30-31] approach or using symmetry-adapted spherical harmonics.[32] Other effects such as incorrect intensities due to extreme texture or a small number of large grains in the sample can be harder or impossible to model. In these cases the only solution is to obtain better experimental data.

One common oversight is not using the correct LP correction for the instrument in question. This will lead to systematic errors in intensity with q which often shows up in unreasonable atomic displacement parameters.

6. Agreement factors and visually assessing refinements

The progress of a Rietveld analysis is usually monitored using various agreement or R-factors which are related to the quantities minimized discussed in Section 2. One is the profile R-factor,[33] which measures the numerical difference between the measured and calculated profile:

$$R_p = \frac{\sum_{i=1}^{N} \left| y_{obs,i} - y_{calc,i}(\mathbf{p}) \right|}{\sum_{i=1}^{N} y_{obs,i}} \qquad \text{(Eq. 21)}$$

R_p can overemphasize the strong reflections and it does not take experimental uncertainties into account. R_{wp} (wp = weighted profile) includes the weighting scheme, and is directly related to the Rietveld objective function (Eq. 2):

$$R_{wp} = \sqrt{\frac{\sum_{i=1}^{N} w_i \left(y_{obs,i} - y_{calc,i}(\mathbf{p}) \right)^2}{\sum_{i=1}^{N} w_i y_{obs,i}{}^2}} \qquad \text{(Eq. 22)}$$

Both these agreement factors include the background portions of the pattern. When the background is high they can be low even if the fit to the diffraction peaks is poor. To avoid this problem, it is useful to subtract the background from the observed step scan intensities in the denominator:

$$R'_{wp} = \sqrt{\frac{\sum_{i=1}^{N} w_i \left(y_{obs,i} - y_{calc,i}(\mathbf{p}) \right)^2}{\sum_{i=1}^{N} w_i \left(y_{obs,i} - Bkg_i \right)^2}} \qquad \text{(Eq. 23)}$$

Another issue associated with profile R-values is that they cannot be readily compared with patterns obtained under different conditions. It is therefore challenging to define what is a "good" R-value.[33] One way round this is via the so-called expected R-factor, which is wholly determined from counting statistics, and gives a measure of the best possible fit.

$$R_{exp} = \sqrt{\frac{N-P}{\sum_{i=1}^{N} w_i y_{obs,i}{}^2}} \approx 1/\sqrt{\langle y_{obs,i}\rangle} \qquad \text{(Eq. 24)}$$

or:

$$R'_{exp} = \sqrt{\frac{N-P}{\sum_{i=1}^{N} w_i \left(y_{obs,i} - Bkg_i\right)^2}} \approx 1/\sqrt{\langle y_{obs,i} - Bkg_i\rangle} \qquad \text{(Eq. 25)}$$

for *N* data points and *P* parameters. If $y_{obs,i}$ are raw counts, then R_{exp} and R'_{exp} are, respectively, approximately the inverse of the square root of the average observed count and the average (observed−background) count.

The ratio χ between R_{wp} and R_{exp} (also called the goodness of fit GOF) is a measure of the quality of fit:

$$\chi = \frac{R_{wp}}{R_{exp}} = \sqrt{\frac{\sum_{i=1}^{N} w_i \left(y_{obs,i} - y_{calc,i}(\mathbf{p})\right)^2}{N-P}} \qquad \text{(Eq. 26)}$$

A χ between 1 and 1.5 usually indicates a good model. Note that χ^2 is the function that is being minimised. By definition, a χ valued less than 1 is a statistical impossibility. Low values of χ can occur if you have a high background (R_{wp} will be artificially low) or a high value of R_{exp} due to insufficient counting times.

For a more direct comparison with single crystal data, R_{Bragg} can be used, which is based on integrated reflection intensities rather than step scan intensities:

$$R_{Bragg} = \frac{\sum_{k=1}^{K} \left|I_{obs,k} - I_{calc,k}\right|}{\sum_{k=1}^{K} I_{obs,k}} \qquad \text{(Eq. 27)}$$

$I_{obs,k}$ and $I_{calc,k}$ are the "observed" and calculated intensities of the kth out of *K* reflections. Rietveld R_{Bragg} values are often much lower than those from single crystal experiments and should be interpreted with caution. When peaks overlap, the total intensity is apportioned to individual *hkl*-reflections according to the ratio of the calculated intensities. This leads to a biased or overly optimistic assessment of R_{Bragg}.

The Durbin-Watson[34-35] statistic:

$$d = \frac{\sum_{i=1}^{N}(\Delta y_i - \Delta y_{i-1})}{\sum_{i=1}^{N}(\Delta y)^2} \qquad \text{(Eq. 28)}$$

with $\Delta y_i = y_{obs,i} - y_{calc,i}$ measures serial correlations between adjacent data points in the difference pattern. For a good refinement in which the difference plot is random, a value of 2.0 is expected. Correlated uncertainites lead to significantly lower values.

In practice, the best way to judge a refinement is often via a Rietveld plot such as Figure 1. Here the observed, calculated and difference profiles are shown and visual analysis of these can often identify problems with the model. Some practical points to consider include:

- Look at plots on y_{obs}, $\sqrt{y_{obs}}$ and $\ln y_{obs}$ scales to identify problems with both weak and strong peaks.
- Plot the background function to make sure it is appropriate, particularly with structure-independent refinements at high q where there is significant peak overlap.

- Make sure the fit is good over the whole *X* range.
- Look at both the difference and weighted difference curves for systematic problems as a function of *X*. Small misfits of weaker peaks may be more statistically important than larger misfits on strong peaks due to the $1/\sigma(y_{obs,i})^2$ weighting. The weighted difference plot also puts the discrepancies on a statistically meaningful scale.
- Plot the cumulative χ^2 function[36] which shows the contributions to χ^2 as a function of *X* to identify problem regions of the fit.
- A poor WPPF fit can be masked by plotting over a large *X* range, by using a *y* scale that emphasizes only the strong reflections, or by using large points for the experimental data. Do not do this in presentations or publications!
- When describing a refinement never say you "refined the data". The parameters are refined; the data are fitted.

7. Multiphase and multipattern

Most of the discussion above has focused on fitting a single powder pattern containing a single crystalline phase. However, as shown by Eq. 1, it is straightforward to extend the method to multiphase samples. One can then analyse multiple structures simultaneously. In the case of Rietveld refinement one can obtain quantitative information on the crystalline phases present via the Rietveld scale factors. By using internal intensity standards, information on the amorphous content of a sample can also be obtained.

It is also common to have more than one powder pattern for a given sample. In the case of time-of-flight neutron diffraction, the data are normally collected from different banks of detectors giving several powder patterns which cover different *d*-spacing ranges with different resolutions. It is common to fit these data simultaneously with a single structural model in a "multi-bank" or "multi-histogram" refinement. It can also be useful to simultaneously fit data from multiple sources using a single structural model. The most common application is a combined X-ray and neutron refinement. Here one takes advantage of the different scattering factors (lengths) of X-rays and neutrons to gain more information on a material. Simultaneous fitting of powder diffraction data and PDF data (see the lecture from Prof. Billinge) or powder data and data from other techniques such as XAFS is also possible.

Procedures for analysing multiple data sets from a single sample under evolving conditions (time, temperature, pressure, chemistry, etc.) are covered in later notes.

8. Refinement strategy

In the early days of WPPF it was crucial to adopt a conservative refinement strategy to prevent the least squares diverging. With modern software many of these issues have disappeared. However, some general points for problem refinements include:

- Before refining any parameters, visually compare the observed and calculated patterns (perform zero least squares cycles) to identify the most important discrepancies.
- Don't be afraid to change parameters to more sensible values and perhaps fix them during early stages of the refinement.
- A refinement is unlikely to converge if there is no overlap between calculated and observed peaks in cycle zero.
- Peak-shape parameters are often highly correlated. Consider starting with a fixed peak shape, or one with a small number of free parameters.

- In Rietveld work consider initially fixing cell parameters and peak shapes at values derived from a Pawley or Le Bail fit.
- Try using a restricted 2θ range in early stages of the refinement. This speeds up calculations, and the smaller number of reflections at lower angles makes it easier to identify potential problems.
- Remember to turn on all relevant parameters for the final cycles of refinement to ensure that parameter uncertainties are calculated correctly.
- Examine the uncertainties in parameters using the variance-covariance matrix. Don't arbitrarily fix one parameter to remove correlation problems if the parameters are of interest.
- Be careful if your software has "helped you" by setting an artificial minimum and maximum limit on a parameter and that limit has been hit. Fix the problem or remove the parameter so the values and uncertainties of other parameters are correctly calculated.
- Save all the details of your model and final refinement in a full powder CIF file (see later lectures).
- Never refine a parameter if you do not know what it does. Not every "tick box" option needs to be ticked and, in TOPAS, not every ! should be an @.

9. Conclusions and what next

There are several workshops where you can learn different Rietveld packages (FullProf, GSAS, TOPAS) from the experts. Each package has different strengths and weaknesses; knowing the tricks available in each is useful. For a simple practical introduction to Rietveld refinement you could try "Structure Analysis from Powder Diffraction Data: Rietveld Refinement in Excel".[37] This paper introduces least squares refinement using the solver function in Excel, as well as guiding you through solving a linear least squares problem by hand. It then discusses fitting individual peaks in a pattern, building from this towards a Pawley-like fit, then a full Rietveld refinement of a simple structure. There is an accompanying online tutorial at https://topas.webspace.durham.ac.uk/tutorial_riet_excel/. Website https://topas.webspace.durham.ac.uk/topas_user_menu/ has various training exercises in the methods discussed. Finally there are post-school "ask the expert" opportunities via the Rietveld mailing list (rietveld_l-request@ill.fr) or user forums (e.g. https://topas.awh.durham.ac.uk/flarum/public/).

10. Acknowledgements

Parts of these notes follow the discussion in "Rietveld Refinement" by Robert Dinnebier, Andreas Leineweber and John S.O. Evans. We thank Andreas for helping us formulate those sections.

11. References

1. Rietveld, H. M., Line Profiles of Neutron Powder-Diffraction Peaks for Structure Refinement. *Acta Crystallographica* **1967,** *22* (1), 151-152.
2. Rietveld, H. M., A Profile Refinement Method for Nuclear and Magnetic Structures. *Journal of applied Crystallography* **1969,** *2* (2), 65-71.
3. Pawley, G., Unit-cell Refinement from Powder Diffraction Scans. *Journal of Applied Crystallography* **1981,** *14* (6), 357-361.
4. Le Bail, A., Whole Powder Pattern Decomposition Methods and Applications: A Retrospection. *Powder Diffraction* **2005,** *20* (4), 316-326.
5. Le Bail, A.; Duroy, H.; Fourquet, J., *Ab-initio* Structure Determination of $LiSbWO_6$ by X-ray Powder Diffraction. *Materials Research Bulletin* **1988,** *23* (3), 447-452.
6. Dinnebier, R. E.; Billinge, S. J., *Powder Diffraction: Theory and Practice*. Royal Society of Chemistry: 2008; p 574.

7. Dinnebier, R. E.; Leineweber, A.; Evans, J. S. O., *Rietveld Refinement, Practical Powder Diffraction Pattern Analysis using TOPAS*. De Gruyter: 2018; p 331.
8. Pecharsky, V.; Zavalij, P., *Fundamentals of Powder Diffraction and Structural Characterization of Materials*. Springer Science & Business Media: 2008.
9. Rietveld, H. M., The Rietveld method. *Physica Scripta* **2014,** *89* (9), 098002.
10. van Laar, B.; Schenk, H., The Development of Powder Profile Refinement at the Reactor Centre Netherlands at Petten. *Acta Crystallographica Section A: Foundations and Advances* **2018,** *74* (2), 88-92.
11. Young, R. A., *The Rietveld Method*. Oxford University Press: 1993.
12. McCusker, L.; Von Dreele, R.; Cox, D.; Louër, D.; Scardi, P., Rietveld Refinement Guidelines. *Journal of Applied Crystallography* **1999,** *32* (1), 36-50.
13. Prince, E., Mathematical aspects of Rietveld Refinement. In *The Rietveld Method*, OUP: Oxford, 1993; pp 43-54.
14. von Dreele, R. B., Rietveld Refinement. In *Powder Diffraction: Theory and Practice*, Royal Society of Chemistry: 2008; pp 266-281.
15. Egami, T.; Billinge, S. J., *Underneath the Bragg peaks: structural analysis of complex materials*. Elsevier: 2003.
16. Neder, R. B.; Proffen, T., *Diffuse Scattering and Defect Structure Simulations: A cook book using the program DISCUS*. OUP Oxford: 2008; Vol. 11.
17. Caglioti, G.; Paoletti, A.; Ricci, F., Choice of collimators for a crystal spectrometer for neutron diffraction. *Nuclear Instruments* **1958,** *3* (4), 223-228.
18. Thompson, P.; Cox, D.; Hastings, J., Rietveld refinement of Debye–Scherrer synchrotron X-ray data from Al_2O_3. *Journal of Applied Crystallography* **1987,** *20* (2), 79-83.
19. Klug, H. P.; Alexander, L. E., *X-ray diffraction procedures: for polycrystalline and amorphous materials*. 1974.
20. Kern, A.; Coelho, A.; Cheary, R., Convolution based profile fitting. In *Diffraction analysis of the microstructure of materials*, Springer: 2004; pp 17-50.
21. Cheary, R. W.; Coelho, A. A.; Cline, J. P., Fundamental parameters line profile fitting in laboratory diffractometers. *Journal of Research of the National Institute of Standards and Technology* **2004,** *109* (1), 1.
22. Cheary, R. W.; Coelho, A. A., Axial divergence in a conventional X-ray powder diffractometer. I. Theoretical foundations. *Journal of Applied Crystallography* **1998,** *31* (6), 851-861.
23. Cheary, R. W.; Coelho, A., A fundamental parameters approach to X-ray line-profile fitting. *Journal of Applied Crystallography* **1992,** *25* (2), 109-121.
24. Cheary, R.; Coelho, A., Axial divergence in a conventional X-ray powder diffractometer. II. Realization and evaluation in a fundamental-parameter profile fitting procedure. *Journal of Applied Crystallography* **1998,** *31* (6), 862-868.
25. Bergmann, J.; Kleeberg, R.; Haase, A.; Breidenstein, B. In *Advanced fundamental parameters model for improved profile analysis*, Materials science forum, Trans Tech Publ: 2000; pp 303-308.
26. Popa, N., The (hkl) dependence of diffraction-line broadening caused by strain and size for all Laue groups in Rietveld refinement. *Journal of Applied Crystallography* **1998,** *31* (2), 176-180.
27. Stephens, P. W., Phenomenological model of anisotropic peak broadening in powder diffraction. *Journal of Applied Crystallography* **1999,** *32* (2), 281-289.
28. Coelho, A. A.; Evans, J. S. O.; Lewis, J. W., Averaging the intensity of many-layered structures for accurate stacking-fault analysis using Rietveld refinement. *Journal of Applied Crystallography* **2016,** *49*, 1740-1749.
29. David, W. I., On the equivalence of the Rietveld method and the correlated integrated intensities method in powder diffraction. *Journal of Applied Crystallography* **2004,** *37* (4), 621-628.
30. March, A., Mathematische Theorie der Regelung nach der Korngestah bei affiner Deformation. *Zeitschrift für Kristallographie-Crystalline Materials* **1932,** *81* (1-6), 285-297.

31. Dollase, W., Correction of intensities for preferred orientation in powder diffractometry: application of the March model. *Journal of Applied Crystallography* **1986,** *19* (4), 267-272.
32. Järvinen, M., Application of symmetrized harmonics expansion to correction of the preferred orientation effect. *Journal of Applied Crystallography* **1993,** *26* (4), 525-531.
33. Toby, B. H., R factors in Rietveld analysis: How good is good enough? *Powder diffraction* **2006,** *21* (1), 67-70.
34. Durbin, J.; Watson, G. S., Testing for serial correlation in least squares regression. III. *Biometrika* **1971,** *58* (1), 1-19.
35. Hill, R.; Flack, H., The use of the Durbin–Watson d statistic in Rietveld analysis. *Journal of Applied Crystallography* **1987,** *20* (5), 356-361.
36. David, W., Powder diffraction: least-squares and beyond. *Journal of Research of the National Institute of Standards and Technology* **2004,** *109* (1), 107.
37. Evans, J. S. O.; Evans, I. R., Structure Analysis from Powder Diffraction Data: Rietveld Refinement in Excel. *Journal of Chemical Education* **2021,** *98* (2), 495-505.